

Biophysical dissection of schistosome septins: insights into oligomerization and membrane binding

Ana Eliza Zeraik¹, Margarita Staykova², Marina Gabriel Fontes¹, Indrè Nemuraité², Roy Quinlan³, Ana Paula Ulian Araújo¹, Ricardo DeMarco¹

¹Instituto de Física de São Carlos, Universidade de São Paulo, São Carlos, SP, Brazil.

²Department of Physics, University of Durham, UK

³School of Biological and Biomedical Sciences, University of Durham, UK

ABSTRACT

Septins are GTP-binding proteins that are highly conserved among eukaryotes and which are usually membrane-associated. They have been linked to several critical cellular functions such as exocytosis and ciliogenesis, but little mechanistic detail is known. Their assembly into filaments and membrane binding properties are incompletely understood and that is specially so for non-human septins where such information would offer therapeutic potential. In this study we use *Schistosoma mansoni*, exhibiting just four septin genes, as a simpler model for characterizing the septin structure and organization. We show that the biochemical and biophysical properties of its *SmSEPT5* and *SmSEPT10* septins are consistent with their human counterparts of subgroups SEPT2 and SEPT6, respectively. By succeeding to isolate stable constructs comprising distinct domains of *SmSEPT5* and *SmSEPT10* we were able to infer the influence of terminal interfaces in the oligomerization and membrane binding properties. For example, both proteins tended to form oligomers interacting by the N- and C-terminal interfaces in a nucleotide independent fashion but form heterodimers via the G interface, which are nucleotide dependent. Furthermore, we report for the first time that it is the C-terminus of *SmSEPT10*, rather than the N-terminal polybasic region found in other septins, that mediates its binding to liposomes. Upon binding we observe formation of discrete lipo-protein clusters and higher order septin structures, making our system an exciting model to study interactions of septins with biological membranes.

1. Introduction

Septins are filament forming GTP-binding proteins highly conserved in eukaryotes [1]. First described in yeast cytokinesis [2], septins were subsequently linked to various processes occurring at the cell cortex, such as exocytosis [3], membrane compartmentalization [4, 5], scaffold assembly [6], ciliogenesis [7], neurogenesis [8] and others [9]. Given this functional diversity, it is not surprising that abnormal septin expression is linked to numerous diseases including neurodegenerative disorders such as Alzheimer's and Parkinson's disease [9, 10].

Since the discovery of septins in yeasts, seminal work on the assembly of septin subunits have been performed in *Saccharomyces cerevisiae* [11]. Among the metazoans, most of the scientific research has been focused on human septins [12-15]. The large number of septin gene in humans can be classified into four phylogenetic subgroups: SEPT2, SEPT7, SEPT6 and SEPT3 [16], which have been further applied to other metazoan organisms [1]. Septin assembly into filaments and higher-order structures such as rings and bars requires hetero-oligomeric complexes, particularly canonical hexamer or octamer in mammals, formed by septins from different subgroups [14, 17]. Theoretically, each member of each subgroup, except SEPT7, is interchangeable in the septin filament to produce variant forms of the canonical complex [16]. Despite the significant progress in the field, the structural and functional characterization of human septins remains extremely challenging due to the polydisperse nature of their assembled structures combined with little detail on what governs septin polymerization into higher order structures, and the importance of GTP binding and hydrolysis. Furthermore, although septins are found predominantly at the cell cortex, the mechanisms that promote their plasma membrane assembly remain mostly elusive and recent studies on the field are just begging to shed light on such mechanisms [18]. Data on the specificity of septins to phosphoinositides and the region of the protein that promotes membrane binding are still scarce (Reviewed by [19]).

Here we focus on the septins found in *Schistosoma mansoni*, the major species responsible for the neglected disease schistosomiasis in America [20]. *S. mansoni* contains only four septin genes, named with respect to their similarity to human septins- *SmSEPT5*, *SmSEPT10*, *SmSEPT7.1* and *SmSEPT7.2*[21]. As we have previously shown, Schistosome septins can also form heterocomplexes capable of filament assembly, which formed curved and straight bundles as described for other species [6, 22].

The goal of this paper is to increase our understanding on the self-assembly of septins, their stability and membrane interactions. For the purpose we undertake a comprehensive biophysical analysis of *SmSEPT10* and *SmSEPT5* proteins from *S. mansoni*. Using recombinantly expressed and purified proteins, we have investigated the role of the N- and C- domains in the oligomerization and membrane binding properties of these septins and show for the first time that it is the C-terminus, rather than the N-terminal polybasic region found in other septins, of *SmSEPT10* that mediates its binding to liposomes.

2. Methods

2.1. Expression and Purification of *SmSEPT5*, *SmSEPT10* and its GTP-binding domains

The cloning, expression and purification of *SmSEPT10*, *SmSEPT10G* and *SmSEPT5* was performed as described elsewhere [21]. *SmSEPT5G* comprises the residues 83-358, *SmSEPT10NG* and *SmSEPT10GC* comprises the residues 1-306 and 39-412, respectively. All protein constructs were expressed in *E. coli* Rosetta (DE3) strain by induction with 0.4 mM of IPTG for 16 h at 18 °C and purified by affinity chromatography using Ni-NTA resin followed by size-exclusion chromatography (SEC) using a Superdex 200 column. The integrity and purity of the proteins were confirmed by 15% (w/v) SDS-PAGE. The standard buffer for these proteins was 50 mM Tris-HCl pH 8.0, 300 mM NaCl, 10% (v/v) glycerol, 5 mM β -mercaptoethanol.

2.2. Oligomerization State

The size-exclusion chromatography on Superdex 200 10/30 and the chemical cross-linking were the techniques used to assess the oligomeric state of *SmSEPT10*, *SmSEPT5* and their GTP-binding domains. The apparent molecular weight was determined through a calibration curve using *Gel Filtration Calibration Kits* (GE Healthcare). Results were expressed in K_{av} : [elution volume - column void volume]/[total column volume - column void volume] [23]. For the chemical cross-linking reactions, 10 μ M of *SmSEPT10*, *SmSEPT10G*, *SmSEPT5* and *SmSEPT5G* in buffer 50 mM HEPES pH 8.0, 300 mM NaCl, 10% (v/v) glycerol and 5 mM β -mercaptoethanol were incubated on ice with 0.5, 1.0 and 5 mM of ethylene glycol bis[succinimidylsuccinate] (EGS). Aliquots

were taken after 1, 2 or 4 hours of incubation, the reactions were stopped by adding Tris-HCl pH 8.0 (100 mM final concentration) before adding SDS loading buffer, and the oligomeric state of the proteins were determined on 10% SDS-PAGE.

Hetero-oligomerization was assessed by size exclusion chromatography after mixing *SmSEPT5G* and *SmSEPT10G* (15 μ M) with 45 μ M of GTP, GDP or GTP γ S overnight in low salt buffer (25 mM HEPES pH 8.0, 100 mM NaCl, 10% (v/v) glycerol, 5 mM β -mercaptoethanol) containing 5 mM of MgCl₂.

SmSEPT5 and *SmSEPT10* G interface mutants were produced according to the instructions of QuikChange Site-Direct mutagenesis kit (Agilent Technologies). The resulting proteins were expressed and purified as described for the wild type proteins.

2.3. Circular Dichroism (CD) and Fluorescence Spectroscopy

CD spectra were collected to evaluate the folding and stability of *SmSEPT10* and *SmSEPT5*. The spectra of *SmSEPT10* and *SmSEPT5* (5 μ M) in acetate-borate-phosphate buffer (20 mM) over a pH range 2-12 were collected using a Jasco 815 spectropolarimeter. The spectra were collected in the wavelength range 200-250 nm at 10 °C and were determined as an average of 8 scans. The CD data were presented in terms of mean residue ellipticity [24]. Fluorescence emission measurements also used to evaluate the folding and stability of *SmSEPT10* and *SmSEPT5*, were performed on a spectrofluorimeter model K2 ISS. The tryptophans were excited at 295 nm at 10 °C. Fluorescence emission spectra were recorded from 300 to 450 nm and quantified by the center of spectral mass (CM), calculated using the formula: $CM = \frac{\sum \lambda_i F_i}{\sum F_i}$, where F_i stands for the intensity of fluorescence emitted at wavelength λ_i [25].

2.4 GTP Hydrolysis Assay

The hydrolytic activity assay was performed according to the method described by Seckler et al [26] with minor modifications [27]. Briefly, 15 μ M of *SmSEPT5* was incubated with 3 fold excess of GTP in the presence of 5 mM of MgCl₂ and aliquots were removed in different time intervals and snap frozen in liquid nitrogen. The nucleotides were extracted from the protein samples by treatment with HClO₄ and analyzed by anion exchange chromatography using a Protein Pack DEAE 5 PW 7.5 mm x 7.5 cm column (Waters) driven by a Waters 2695 chromatography system.

2.5. Right-angle light scattering and Thioflavin-T (ThT) binding assays

To monitor possible aggregates formation with increasing temperatures, 5 μM of *SmSEPT10* and *SmSEPT5* in standard buffer were placed onto a cuvette and the light scattered at 350 nm (90° to the incident light beam) was collected during 90 minutes at 15, 30, 37 and 45 $^\circ\text{C}$ on a spectrofluorimeter model K2 ISS. ThT (50 μM) was incubated with 5 μM of either *SmSEPT10* or *SmSEPT5*. The ThT probe was excited at 450 nm and its emission was recorded at 482 nm over 90 minutes at 15, 30, 37 and 45 $^\circ\text{C}$.

2.6. Isothermal Titration Calorimetry (ITC)

The nucleotide binding affinity of *SmSEPT5* was determined using a VP-ITC calorimeter (MicroCal). Measurements were performed at 18 $^\circ\text{C}$ in standard buffer in the presence or absence of 5 mM MgCl_2 . The sample cell was loaded with *SmSEPT5* (10 μM) and the syringe was filled with GTP γS (0.25 mM) or GDP (3 mM). The titration was carried out until the saturation was achieved (35 injections of 5 μL each). The *software* Microcal[®] ITC Origin[™] was used to obtain the dissociation constant (K_d) and enthalpy. Curve fitting was performed assuming one binding site model and the reaction stoichiometry was fixed ($n=1$) to proper curve fitting due to the low affinity observed. This allowed a reliable determination of K even for low affinity interactions [28]. The ITC experiments were repeated at least twice.

2.7. Interaction of *S. mansoni* septins with Giant Unilamellar Vesicles (GUVs)

GUVs were prepared using the standard electroformation protocol [29] from one of the following 4 mM lipid-chloroform mixtures: 1) 94.9 mol% DOPC (1,2-dioleoyl-sn-glycero-3-phosphocholine), 5 mol% PIP2 (phosphatidylinositol-4,5-bisphosphate) and 0.1 mol% of the Rhodamine-DPPE, or 2) 89.9 mol% DOPC, 10 mol% DOPS and 0.1 mol% of the Rhodamine-DOPE. Briefly, 5 μL of the lipid mixture was deposited on the ITO-coated glass to form a thin film, which was dried overnight under vacuum. The electroformation chamber was assembled by two ITO-coated coverslips with the

conductive sites facing each other, and separated by a 3 mm thick teflon gasket. For the electro-swelling of GUVs, the chamber was filled with 1-2.0 mL of 0.5 M solution of sucrose, and connected to a sinusoidal AC electric field of frequency of 10 Hz and amplitude of 1.7 V peak-to-peak for 90 minutes. The freshly formed GUV suspension was further diluted twice in 0.5 M glucose, resulting in a final concentration of 10-20 μM of lipid.

The individual proteins *SmSEPT5* and *SmSEPT10*, the partial constructs *SmSEPT10G* and *SmSEPT10GC*, and the heterocomplex were labeled with Alexa Fluor 488 NHS ester (Life technologies) following the protocols provided by the manufacturer. The excess of the dye was separated using a PD SpinTrap G-25 column (GE Healthcare). The labeled proteins were stored in 50 mM HEPES pH 8.0, 10% (v/v) glycerol, 5 mM β -mercaptoethanol and 300 mM NaCl (for the individual *SmSEPT5* and *SmSEPT10*) or 500 mM NaCl for the heterocomplex (*SmSEPT5-SmSEPT10-SmSEPT7.2*) and were used within 12 hrs.

Immediately prior to the lipid binding experiments, the desired protein in buffer was diluted about 50 times in glucose solution to achieve a solution with osmolarity of 0.5 M that matches the sucrose osmolarity in the GUVs. The protein-glucose solution was then added to the GUV suspension in the observation chamber. The typical lipid and protein concentrations in our experiments were 10-20 μM and 0.1 - 0.2 μM , respectively. The interaction of the septins with the GUVs was imaged with confocal microscope for up to 1hr following the mixing of the protein with the vesicles.

3. Results

3.1. Nucleotide binding and hydrolysis by SmSEPT5

Several alternative constructs of *SmSEPT5* and *SmSEPT10* summarized in Table 1 were expressed in *E. coli* to evaluate the functions of the different regions of the protein for this and all subsequent assays. A preliminary characterization of nucleotide binding for *SmSEPT10*, a catalytically inactive protein, has been previously performed [27] and therefore this aspect was only explored for *SmSEPT5*. The nucleotide content of the purified *SmSEPT5* was analyzed by anion exchange chromatography and no bound

nucleotide was detected after the second round of purification, suggesting a low affinity for the nucleotide (not shown) and justifying the appropriateness of the purified proteins in ITC and GTP hydrolysis experiments.

Table 1.

S. mansoni septins constructs used and their corresponding domains

Construct	Domains	MW (kDa)
<i>SmSEPT5</i>	Full length protein	53.8
<i>SmSEPT5G</i>	GTP-binding	34.8
<i>SmSEPT10</i>	Full length protein	50.5
<i>SmSEPT10G</i>	GTP-binding	33.3
<i>SmSEPT10NG</i>	N terminus and GTP-binding	37.1
<i>SmSEPT10GC</i>	GTP-binding and C terminus	46.2

Isothermal Titration Calorimetry (ITC) experiments showed a higher affinity of *SmSEPT5* for GTP γ S (Figure 1A) than for GDP (Figure 1B; Table 2). Additionally, *SmSEPT5* binding to GTP γ S required the presence of MgCl₂, no binding was detected in the absence of this ion (data not shown), whilst the binding of GDP to *SmSEPT5* was unaffected by the presence of MgCl₂ (not shown).

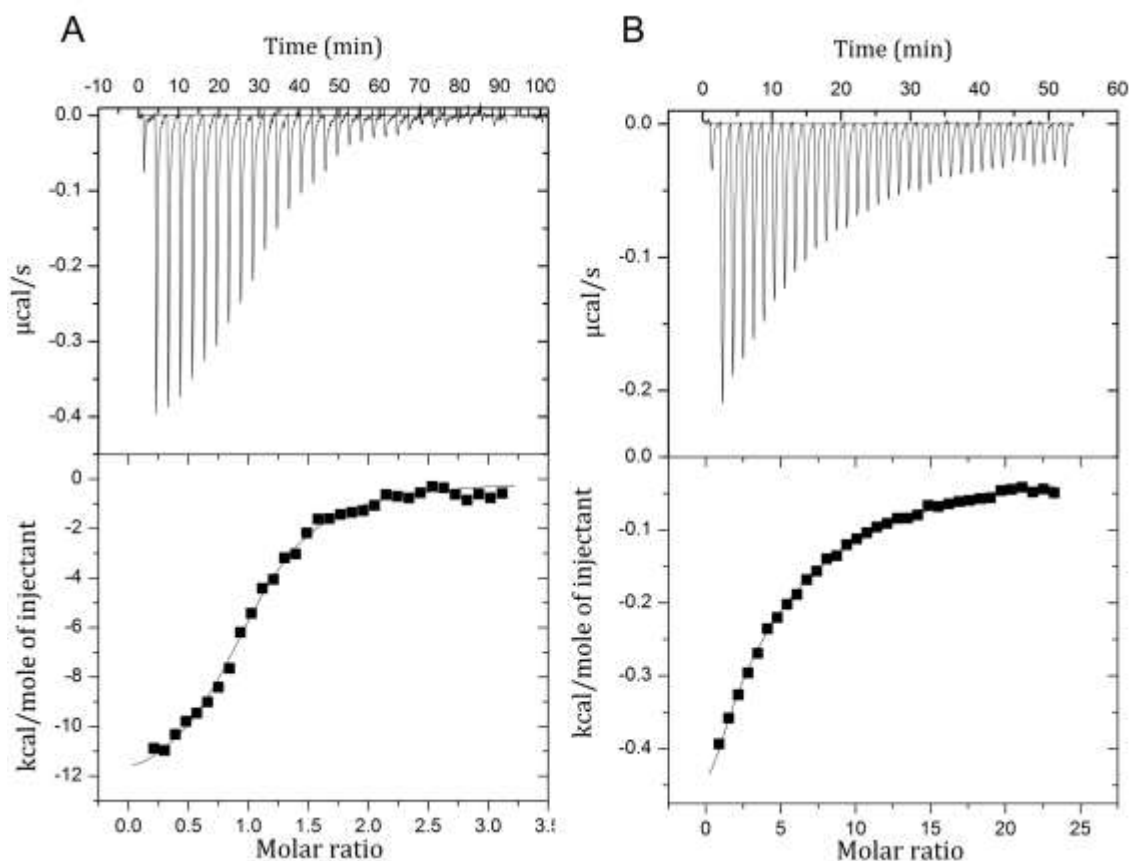


Fig.1. *SmSEPT5* nucleotide binding assay. Raw ITC data (top) and binding isotherms (bottom) from titrations injecting 0.25 μM GTP γS (A) and 3 mM of GDP (B) into the sample cell containing 10 μM of *SmSEPT5* in buffer 50 mM Tris-HCl pH 8.0, 300 mM NaCl, 10% glycerol and 5 mM β -mercaptoethanol. 5 mM MgCl was only included in the buffer of the sample cell for GTP γS titration, since it was determined that ligation of GDP to *SmSEPT5* occurred independent of this co-factor. Each titration was performed until the complete saturation of the binding curve (35 injections of 5 μL of the ligand solutions).

Table 2- Thermodynamic parameters of *SmSEPT5* binding to guanine nucleotides

	K_d (μM)	ΔH (kcal/ mol)
<i>SmSEPT5</i> -GTP γS	1.10 ± 0.08	$-1.29 \pm 0.02 \times 10^4$
<i>SmSEPT5</i> -GDP	155 ± 2	$-4.61 \pm 0.04 \times 10^3$

SmSEPT5 was able to hydrolyze GTP although at relatively low rates (Figure 2). All the GTP was converted to GDP after three to four hours of incubation at 20 $^{\circ}\text{C}$. The presence of the N- and C- domains did not influence the hydrolytic activity of *SmSEPT5*, since the truncated version *SmSEPT5G* displayed the same hydrolysis rate as the full length protein (Figure S1).

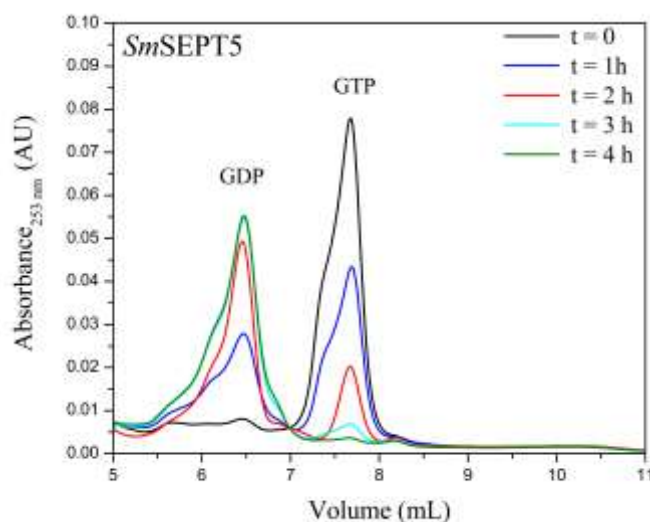


Fig. 2. *SmSEPT5* hydrolyzes GTP. *SmSEPT5* (15 μ M) were incubated with GTP (45 μ M) for 4 h at 20° C, denatured and aliquots of supernatant were taken at different time intervals. Each of the aliquots was separately submitted to anion exchange chromatography and the absorbance at 253 nm, corresponding to absorption wavelength expected from guanine nucleotides, was monitored in the eluate. Peaks observed were labeled as representative of GTP and GDP based on retention times observed for chromatography of standards for each nucleotide in the same conditions.

3.2. *SmSEPT10* and *SmSEPT5* show high stability towards pH changes, but not to high temperatures

The secondary structure of the full-length *SmSEPT10* and *SmSEPT5*, evaluated by Circular Dichroism, remained stable over a wide range of pHs and was affected only at extreme pHs (Figure S2). For example, at pH 12 both spectra presented distortions and at pH 2 we note a slight change in the shape of the spectra, especially evident at the second minimum (at 222 nm). The tertiary structures of the *S. mansoni* septins were evaluated by the fluorescence emission spectra of the tryptophan residues, which were analyzed in terms of the center of spectral mass (CSM). The continuous displacement of the CSM above the pH 10 to higher wavelengths (bathochromic displacement) indicated an increase in the exposition of the tryptophan residues to the solvent [30] and therefore an alteration in the structure of the native proteins (Figure S2 inset) only at highly basic pHs. Taken together, this data indicated that the *SmSEPT5* and *SmSEPT10* display stable secondary and tertiary conformations under a wide range of pH conditions.

Both *SmSEPT5* and *SmSEPT10* were, however, markedly temperature sensitive, with aggregate formation at slightly elevated temperatures. Right-angle light scattering analyses have shown that at 15 °C both septins presented very little variation in the amount of scattered light over time, indicating little particle size variation in solution (Figure 3A and B). In contrast, at temperatures of 37 °C and 45 °C there is a very rapid increase in the amount of scattered light, which indicates the formation of large size aggregated particles for both proteins. *SmSEPT5* were even more sensitive to temperature increase than *SmSEPT10*, presenting increase in the scattered light above 30 °C, while *SmSEPT10* started to aggregate from 37 °C (Figure 3A and B).

The fluorescence of *SmSEPT5* and *SmSEPT10* upon incubation with Thioflavin-T (ThT) probe was monitored over time in different temperatures. ThT is a probe often used to detect β -amyloid-like structures and display an increased fluorescence when interacting with amyloid structures [31, 32]. After a short lag phase, a rapid increase in the ThT fluorescence was observed for *SmSEPT5* above 30 °C (Figure 3C) and for *SmSEPT10* above 37 °C (Figure 3D), indicating that the aggregates formed by these two *S. mansoni* septins with increasing temperatures might include amyloid-like structures.

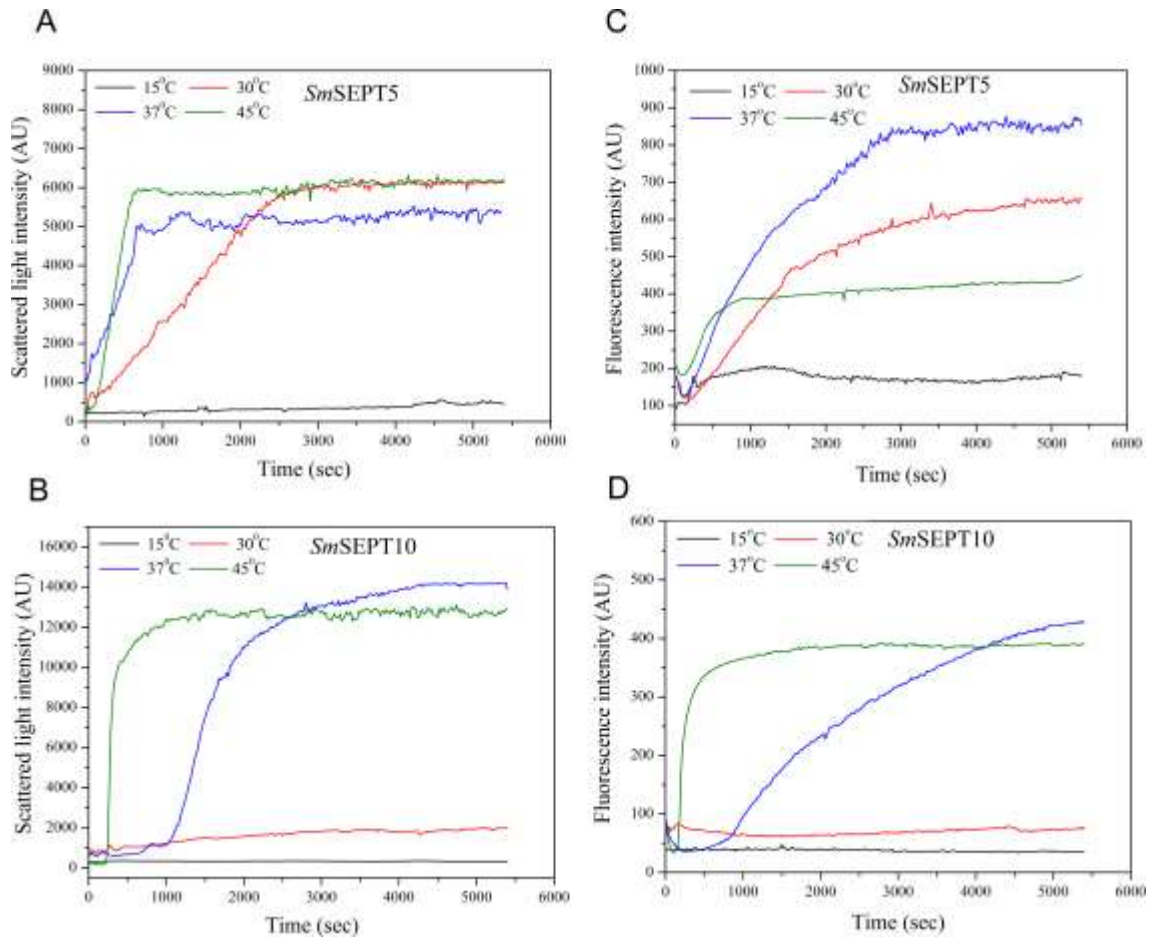


Fig. 3. Temperature effects on the self-assembly of *S. mansoni* septins. Right-angle light scattering of 5 μM of *SmSEPT5* (A) and *SmSEPT10* (B) at different temperatures (15, 30, 37 and 45 $^{\circ}\text{C}$) as a function of time. Fluorescence emission of 50 μM ThT incubated with 5 μM of *SmSEPT5* (C) and *SmSEPT10* (D) at 484 nm ($\lambda_{\text{exc.}} = 450$ nm) in different temperatures for 90 min.

3.3. N- and C- terminal domains influence the oligomerization of *S. mansoni* septins

By analytical SEC, *SmSEPT5* was eluted as a single peak, with an estimated mass of 116 kDa (Figure 4A). This is consistent with it forming a dimer. Further analysis of the oligomeric state by cross-linking experiments also revealed the presence of dimeric forms for the full length *SmSEPT5* (Figure 4B). In contrast, the *SmSEPT5G* construct presented an apparent molecular weight consistent with a monomer (~ 35 kDa) by both SEC (Figure 4C), and cross-linking experiments (Figure 4D).

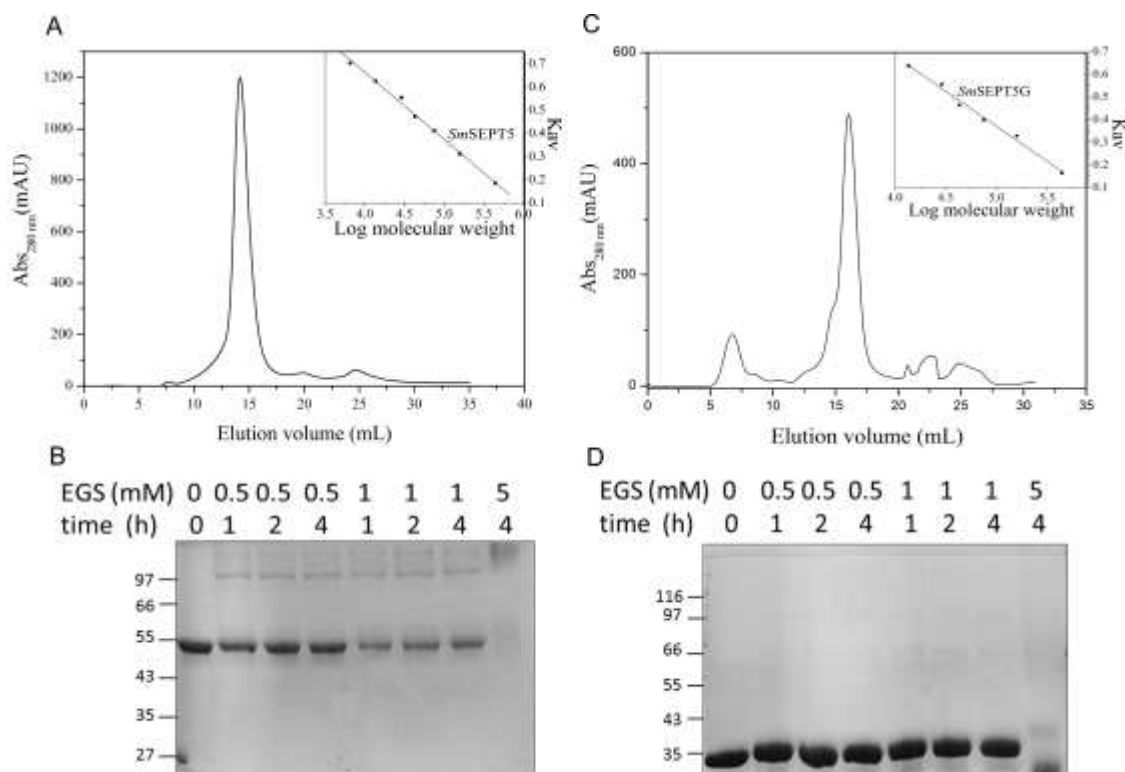


Fig. 4. Influence of N- and C-terminal domains in the oligomeric state of *SmSEPT5*. Size-exclusion chromatograms for *SmSEPT5* (A) and *SmSEPT5G* (C) fractionated on a Superdex 200 column. The right insets show the determination of apparent molecular mass of the proteins from the standard curve using linear regression. The standard proteins of known molecular weight were: Ferritin (440 kDa), Aldolase (158 kDa), Conalbumin (75 kDa), Ovalbumin (44 kDa), Carbonic Anhydrase (29 kDa), Ribonuclease (13,7 kDa) and Aprotinin (6,5 kDa). SDS-PAGE from chemical cross-linking reactions of 10 μ M *SmSEPT5* (B) and *SmSEPT5G* (D) over a 4 hour time course with increasing amounts of EGS (0-5 mM).

SmSEPT10 has shown a single peak in SEC with an apparent mass of 193 kDa (Figure 5A), which would be an intermediate value between a trimer and a tetramer. In contrast, the cross-linking reactions (Figure 5B) show a main band compatible with a dimeric form of this protein (101 kDa).

SmSEPT10G eluted with an estimated molecular weight of 36 kDa, which we interpret as a monomer. A minor peak was also detected, and that would be compatible with a dimer (Figure 5C). Cross-linking of *SmSEPT10G* confirmed the prevalent monomeric form of *SmSEPT10G* in solution (Figure 5D). *SmSEPT10NG* and *SmSEPT10GC* eluted with apparent masses of 43 and 148 kDa, respectively, as determined by SEC (Figure S3), corresponding to monomers for *SmSEPT10NG* and trimers for *SmSEPT10GC*.

To further investigate the role of the NG and G interfaces in the homooligomerization, mutants in conserved positions of the G interface previously shown to be essential for

dimerization [14, 33] were produced. No difference in the apparent mass was observed for the *SmSEPT5* mutants V157D, W309A or Y204D when compared to *SmSEPT5* wild type. Similar results were obtained for *SmSEPT10* mutants T157D, W256A or H267D (Figure S4), suggesting that the G interfaces do not have a role in homooligomeric assembly.

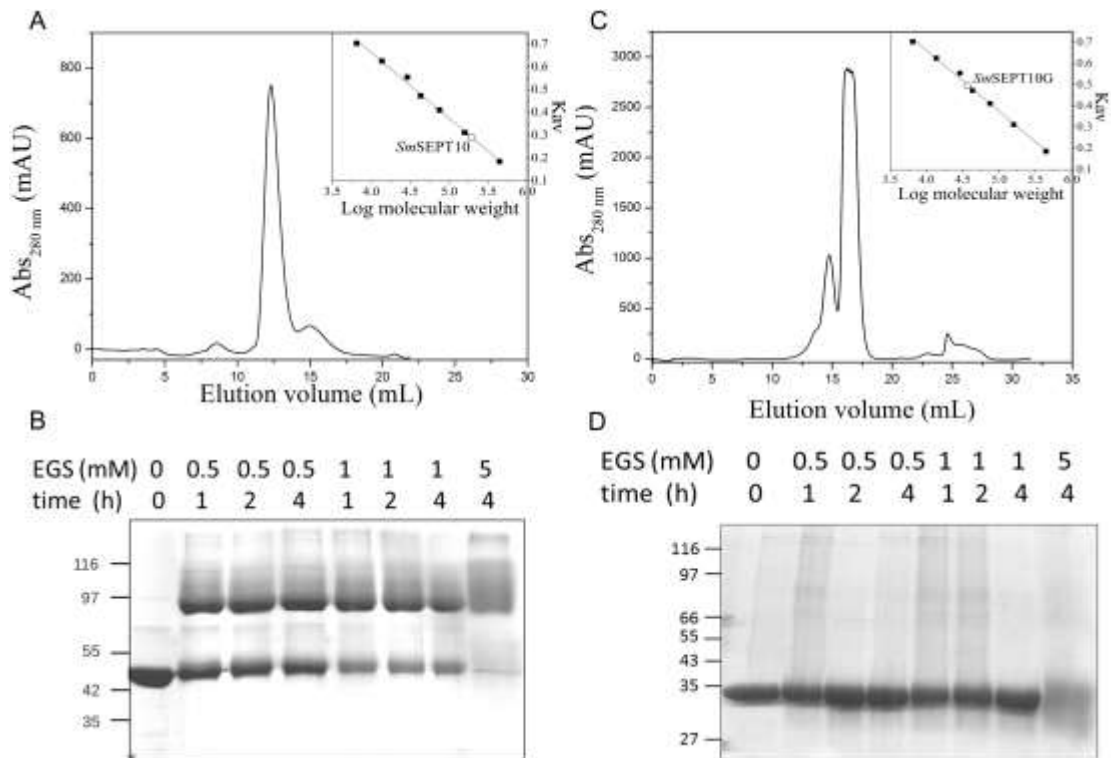


Fig. 5. Influence of N- and C-terminal domains in the oligomeric state of *SmSEPT10*. Size-exclusion chromatograms for *SmSEPT10* (A) and *SmSEPT10G* (C) on a Superdex 200 column. The right insets show the determination of apparent molecular mass of the proteins from the standard curve using linear regression, using the same standards described in the legend of Figure 4. SDS-PAGE from chemical cross-linking reaction of 10 μ M *SmSEPT10* (B) and *SmSEPT10G* (D). A time course reaction (0-4 h) with increasing amounts of EGS (0-5 mM) was performed.

It has been reported that both the ionic strength and guanine nucleotides influence the oligomerization of some septins [33-35]. *SmSEPT10G* was incubated with GDP and GTP in low salt concentration (100 mM NaCl) and subjected to SEC. Neither the presence of the nucleotides nor the low salt concentration influenced the oligomeric state of *SmSEPT10G* (Figure S5). The oligomeric form of full length *SmSEPT5* and *SmSEPT10* as well as *SmSEPT5G*, *SmSEPT10NG* and *SmSEPT10GC* were also

unaffected by incubation with guanine nucleotides, low salt concentration or alkaline phosphatase treatment (not shown).

In contrast, heterooligomers formed by mixing *SmSEPT5G* and *SmSEPT10G* were only formed when those two proteins were incubated with GTP, GDP or GTP γ (Figure 6). Additionally, it was observed that the proportion of protein dimerized was very dependent on which nucleotide was added, with GTP being the more efficient to promote protein dimerization (Figure 6).

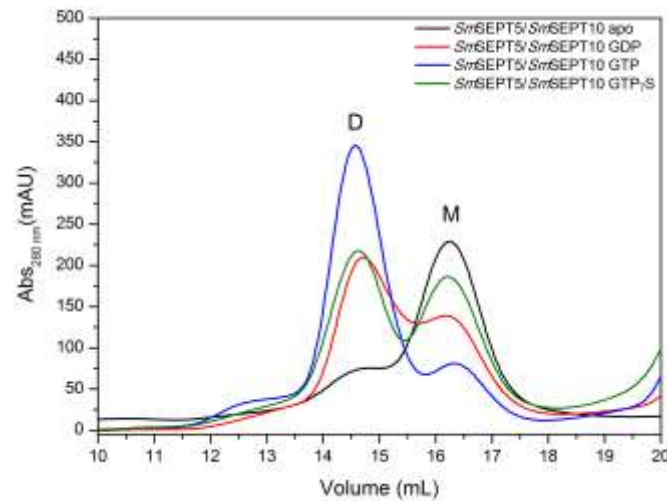


Fig. 6. *SmSEPT5G* and *SmSEPT10G* undergo heterodimerization in the presence of guanine nucleotides. Size exclusion chromatography on a Superdex 200 column. *SmSEPT5G* and *SmSEPT10G* were incubated overnight in the absence (black curve) and in the presence of three fold excess of GDP (red), GTP (blue) or GTP γ S (olive), the monomer-dimer equilibrium shifts toward the heterodimer in the presence of guanine nucleotides. D, dimer; M, monomer.

3.4. *S. mansoni* septin interaction with model membranes

We have assessed the capacity of *S. mansoni* septins to bind to lipid membranes by imaging the interaction of the fluorescently labeled septin proteins with giant unilamellar vesicles (GUVs). It has been reported that septins bind to phosphoinositide lipids, specifically to PIP2 (phosphatidylinositol-4,5-bisphosphate), therefore the reference composition of the GUV membrane in our experiments was chosen to be 95 mol% DOPC and 5 mol% PIP2 [36, 37]. Our results show that individual full length *SmSEPT5* and *SmSEPT10* proteins are both able to bind the GUV membrane after a few minutes of incubation. *SmSEPT5* appears homogeneously enriched on the vesicle surface (Figure 7A). In few of the vesicles (less than 10%) formation of protein-lipid

tubular clusters protruding outward of the vesicle is observed (Figure S6). In comparison, *SmSEPT10* exhibits a very characteristic non-homogeneous binding to all vesicles (Figure 7B). It self-assembles into ordered “cage-like” structures on the vesicle membrane (Figure 7C), which in some cases appear to distort the circular shape of the vesicles, thus suggesting a strangling action (Figure 7D).

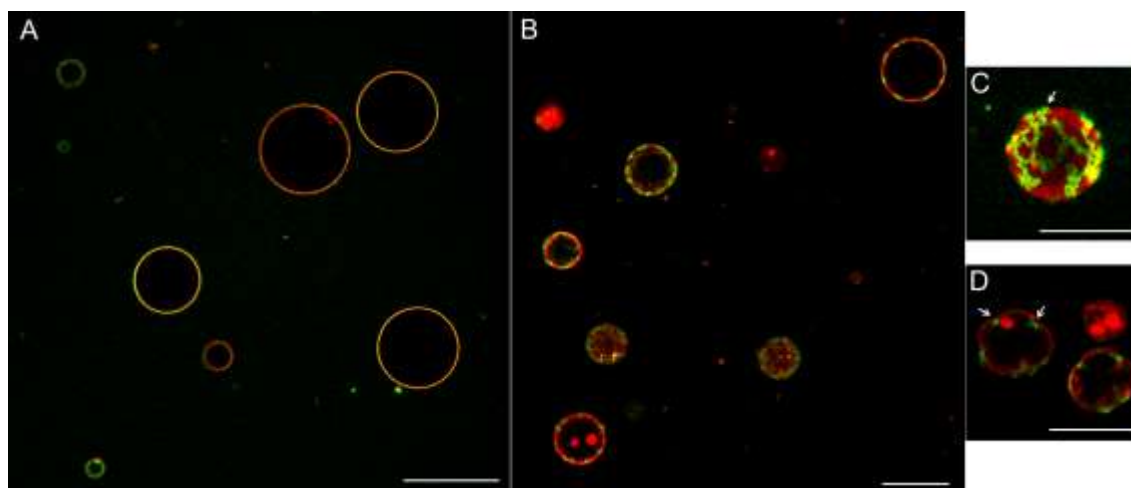


Fig. 7. Individual schistosome septins bind to liposomes. Confocal optical sections of GUVs (94.9 mol% DOPC, 5 mol% PIP2, 0.1 mol% of Rhodamine-DPPE,) (red) incubated with labeled proteins (green). (A) *SmSEPT5* 100 nM binds to GUVs yellow signal can be observed as *SmSEPT5* (green) colocalizes with the labeled lipid (red). (B) *SmSEPT10* (100 nM) is found covering the surface of the GUVs, forming cage-like structures. (C) Higher magnification view of *SmSEPT10* forming organized structures (arrow) all over the GUV surface. (D) *SmSEPT10* is able to promote vesicle deformation; it is possible to note regions of high protein concentration on sites of vesicle deformation (arrows). Scale bar, 30 μm . The images were acquired within the first 10 min of incubation of the septins with the GUVs.

Next we assessed the role of the membrane composition on septin binding. *SmSEPT10* proteins binds equally well to vesicles containing 10 mol% DOPS, which although chemically different contain the same amount of negative charge as the 5 mol% PIP2 vesicles (Figure 8A). *SmSEPT10* does not bind to uncharged DOPC vesicles (Figure 8B) and no binding was detected on 2.5 mol% PIP2 or 5 mol% DOPS containing vesicles (data not shown), suggesting that a critical amount of negative charge is required for the binding process.

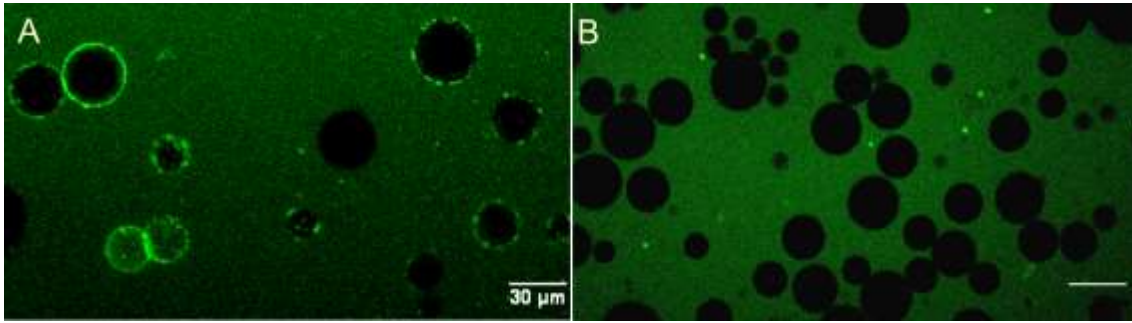


Fig. 8. *SmSEPT10* binds to DOPS but not to DOPC only GUVs. (A) GUVs containing 10 mol% DOPS, 89.9 mol% DOPC, 0.1 mol% of Rhodamine-DPPE imaged after 10 min of incubation with 100 nM of *SmSEPT10*. Binding of *SmSEPT10* to DOPS vesicles can be observed as the enrichment of the protein signal (green) on the surface of the GUV. (B) GUVs composed of 99.9 mol% DOPC, 0.1 mol% of Rhodamine-DPPE incubated with 100 nM of *SmSEPT10*, protein binding was not observed even after 30 min of incubation, which is evident by the lack of green signal on the surface of the GUVs. Scale bar, 30 μm .

To determine which portion of the *SmSEPT10* protein promoted its binding to the lipid membrane we incubated different protein constructs with 5 mol% PIP2/95mol% DOPC vesicles. We detected no enrichment of the G and NG constructs on the vesicle surface (Fig 9A and B), which suggests that the GTP-binding domain and the N- terminus of the *SmSEPT10* protein are not involved in the membrane interaction. The GC construct however readily binds to the vesicle membrane and forms very similar ordered structures as the full length *SmSEPT10* proteins (Figure 9C).

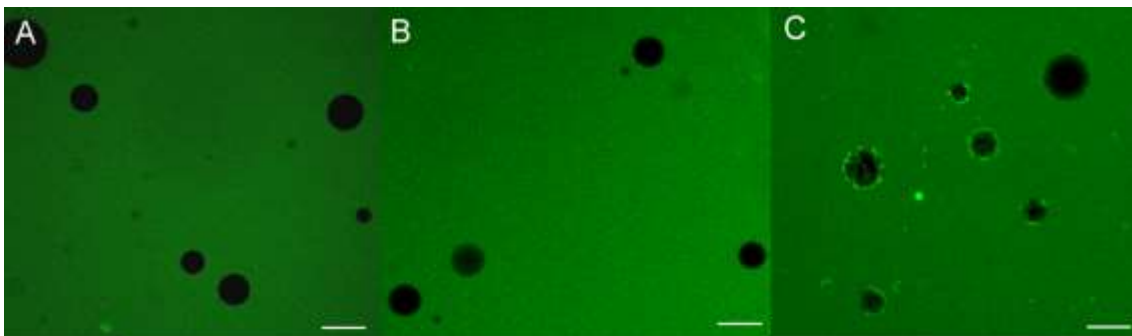


Fig. 9. C-terminus of *SmSEPT10* promotes binding to GUVs. GUVs (94.9 mol% DOPC, 5 mol% PIP2, 0.1 mol% of Rhodamine-DPPE,) incubated with 100 nM of *SmSEPT10G* (A), *SmSEPT10NG* (B) and *SmSEPT10GC* (C). Enrichment of the protein on the vesicle surface was only observed in the presence of the C-terminus of the protein (*SmSEPT10GC*). Scale bar, 30 μm .

Experiments utilizing a previously characterized heterocomplex [22] formed by schistosome SEPT5, 7.2 and 10 also indicated binding of the complex to GUVs

containing PIP2 (Figure 10), but not to pure DOPC vesicles (Figure S7). The binding of the complex results in the formation of lipo-protein aggregates on the surface of most vesicles (Figure 10)

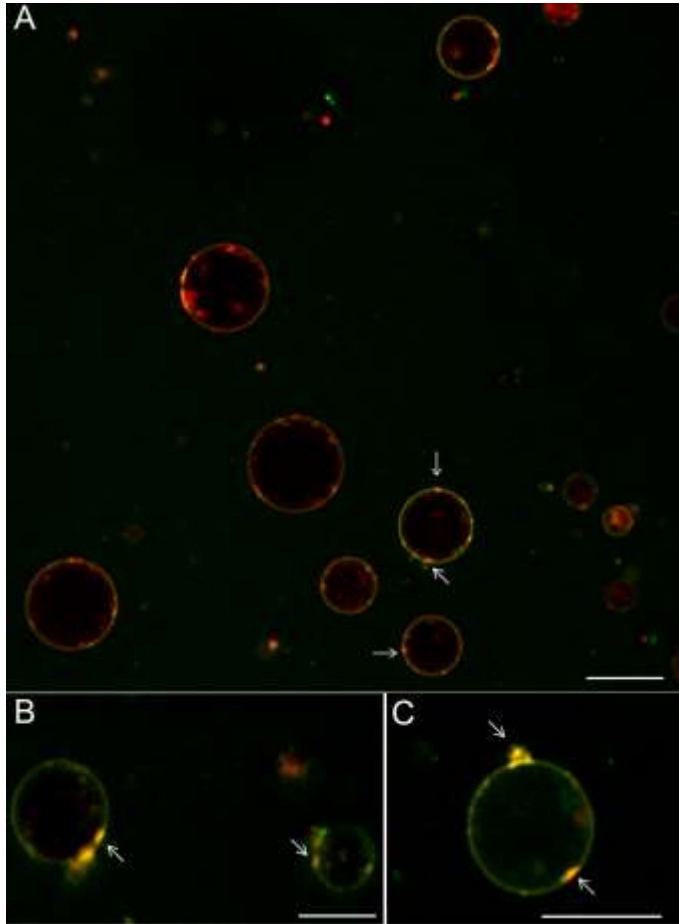


Fig.10. *S. mansoni* septin heterocomplex binds to PIP2-containing GUVs. (A-C) GUVs composed of 94.9 mol% DOPC, 5 mol% PIP2, and 0.1 mol% Rhodamine-DPPE were incubated with 100 nM of *S. mansoni* heterocomplex (*SmSEPT5-SmSEPT10-SmSEPT7.2*) labeled with Alexa Fluor 488 NHS. Figures shows confocal sections of the merged channels (red channel corresponding to the GUV surface and green channel which reflects the distribution of the Septin heterocomplex), confirming the superposition of the GUV surface with the regions of protein accumulation (yellow areas). The arrows point to protein-lipid clusters observed on the surface of the GUVs. (C) is a high magnification view of a GUV containing protein-lipid clusters (arrows). Scale bar, 30 μm.

4. Discussion

Our comparative analysis of *SmSEPT5* and *SmSEPT10* with their human analogues has revealed both new insights and common characteristics between the proteins belonging to SEPT2 and SEPT6 phylogenetic groups, respectively.

The nucleotide binding affinity of *SmSEPT5* and *SmSEPT10* appears consistent with their phylogenetic classification. *SmSEPT5* displays a magnesium dependent high affinity GTP binding and a low affinity magnesium independent GDP binding, which is a trait shared with human SEPT2 [38], and is consistent with a GTPase. The GTP and GDP dissociation constants for *SmSEPT5* differ by two orders of magnitude compared to only one order of magnitude for the human homologue. In comparison, recombinant *SmSEPT10* is unable to hydrolyze GTP, as we have previously shown [27], although it can bind both GTP and GDP. This is consistent with *SmSEPT10* belonging to the SEPT6 subgroup, which is known to lack GTPase activity.

Both full length *SmSEPT-10* and *-5* tend to form homooligomers in solution, however monomers are observed when only the GTP-binding domain is expressed, revealing the importance of the N- and C- terminal domains in the homooligomerization of these proteins. SEC results make difficult to determine if *SmSEPT10* forms a dimer or a higher order complex in solution, but the predicted presence of a large coiled-coil in the C-terminus of this protein makes the SEC results unreliable, since the calibration proteins are primarily globular [23], [39]. Mutations of residues previously shown to be essential to interaction between septins in the G interfaces did not alter the apparent mass of these complex in SEC experiments. Considering that in those mutants each septin would only have a single interface available for interaction with a partner septin, they should represent dimers assembled via the NC interface.

It has been shown that septins that undergo dimerization through the GTP-binding interface are influenced by the presence of GTP or GDP [14, 34, 35]. However, the homooligomers observed for the full length *SmSEPT5* and *SmSEPT10* and their partial constructs appeared insensitive to incubation with nucleotides or treatment with alkaline phosphatase, thus providing further evidence that the homooligomers observed for each of them are probably interacting via the NC interface, rather than the GTP-binding interface.

The presence of the nucleotides, however, have shown to be essential for the heterodimerization of *SmSEPT5G* and *SmSEPT10G*, which interact via the G interface,

as expected for the canonical heterocomplex. Similar conclusion was obtained by Martinez et al. [40], where the deletion of the C or N terminal of the human septins SEPT4, SEPT5 and SEPT8 abolished homotypic assembly of these proteins but not the heterotypic assembly. The higher efficiency of GTP in relation to the non-hydrolyzable GTP γ S in forming heterodimers may indicate that the G interface interaction was formed with *Sm*SEPT5 bound to GDP (after hydrolysis of GTP) and *Sm*SEPT10 bound to GTP (since it lacks GTPase activity), similarly to what was observed for equivalent interface in the canonical human heterocomplex SEPT2/SEPT6/SEPT7 [14]. The fact that monomeric *Sm*SEPT5 displays GTPase activity, despite the lack of an interface between two GTPase domains, is not surprising since previous studies have shown that human septins monomers are capable of hydrolyzing GTP [15]. The biological relevance, if any, of this hydrolytic activity from monomers is still to be determined.

Considering a previously proposed model where *S.mansoni* septins should form a similar heterocomplex to that described for human septins, *Sm*SEPT5 would be expected to occupy the central position in the heterohexamer and an interaction between two *Sm*SEPT5 would occur through the NC-interface. The dimer for this protein observed here would therefore replicate an interface that would be observed in a native filament of the parasite and therefore would be of particular interest for further studies. On the other hand, the NC interaction observed for *Sm*SEPT10 would be a promiscuous one, which is a common behavior for septins expressed in the absence of their proper interaction partners [41].

Analysis of protein stability over pH show very similar profiles for *Sm*SEPT5 and *Sm*SEPT10, with *Sm*SEPT10 CD profile suggesting a more stable structure at extreme alkaline pHs. It was previously shown that formation of salt bridges by positively charged residues tend to contribute to protein stability on very basic pHs [42] and since *Sm*SEPT10 contains a basic region at its C-terminus, which is lacking in *Sm*SEPT5, it is possible that some of the additional positively charged residues on the C-terminus might contribute to protein stability.

Both proteins have the tendency to form amyloid-like aggregates at high temperature, which provides further evidence that these *S. mansoni* septins behave very similarly to their human counterparts [12, 13, 43].

Our data suggests that both the individual septins, *Sm*SEPT5 and *Sm*SEPT10, and the heterocomplex *Sm*SEPT5-*Sm*SEPT10-*Sm*SEPT7.2 are able to interact with lipid membranes, which provides further insights on their functionality. The interaction

requires a certain amount of negatively charged lipids in the membrane, e.g. either PIP2 or DOPS, thus suggesting that this interaction has an important electrostatic component. It has been previously described that septins interact with negatively charged lipids, especially phosphoinositides, through the $\alpha 0$ helix [36]. Such mechanism however cannot be expected for *SmSEPT10*, which lacks the polybasic $\alpha 0$ helix region. In fact, our experiments show that it is the C-terminus that promotes the binding of *SmSEPT10* to the GUV membrane. This novel interaction mechanism between septins and lipid membranes is likely to play a role also in the SEPT6 subgroup in metazoans, which likewise show a highly charged and highly conserved C-terminus (Supplementary Figure S8) and also lack the polybasic helix. Considering that our experiments suggests that both *SmSEPT5* and *SmSEPT10* form homodimers through the NC interface, further studies are necessary to verify if dimer formation could be a significant factor for interaction of the C-terminus with lipids.

The individual septins and the heterocomplex do not only passively bind to lipid vesicles, but are able to self-organize on the lipid membrane and promote its remodeling. For example, upon binding to GUVs the *SmSEPT 5, 7.2 and 10* heterocomplex induces formation of discrete lipo-protein clusters on the vesicles, which however do not elongate into tubules as previously observed by Tanaka-Takiguchi et al. [37]. In contrast, individual *SmSEPT10* proteins are able to self-assemble into characteristic cage-like structures, covering and deforming the whole vesicle. The characteristic lateral arrangement of *SmSEPT10* is likely explained by earlier observations showing that septins filament can interact laterally through their coiled-coils in the C-terminal region [44]. Since *SmSEPT10* protein have a much larger coiled-coil region than the *SmSEPT5* (suggested also by our SEC data), they are more prone to self-organize laterally than the *SmSEPT5* homofilaments (short coiled coils) or *SmSEPT 5, 7.2 and 10* heterofilaments (mixture of long and short coiled-coils), thus explaining their different behaviors on the membrane. It is interesting to note that *SmSEPT10* does not form cage-like structures while in solution, which confirms the crucial role of the lipid bilayer in facilitating the protein interactions.

Our results imply that septins may play a far more active role in the process of exocytosis than the currently proposed regulatory role, mediated through focal septin assemblies on the surface of the emerging secretory vesicle [45-47]. Based on our findings it is tempting to propose that septins form a mesh on the membrane surface that

contributes to the process of membrane deformation and that serves as a scaffold to which other proteins from the exocytotic pathway adhere.

Considering the very diverse tissue localization of septins in the *Schistosoma* life cycle [21], it is expected that septins filaments are very versatile, being involved in several different cellular processes as observed for other models. Therefore, further understating of their properties may help to elucidate mechanism related to several aspects of parasitic lifestyle. Moreover, Schistosome septins constitute a simple model to study general proprieties of Metazoan septins. The model established here for the study of interaction of *S. mansoni* septins with membranes may constitute an important step to permit greater insight in several processes involving those two components.

Author contributions

A.E.Z., M. S., A.P.U.A. and R.D.M. designed the experiments; A.E.Z., M. S., M.G.F. and I.N. performed the experiments; A.E.Z., M.S., M.G.F. and I.N. analyzed the data; A.E.Z., M. S., A.P.U.A., R.Q. and R.D.M. wrote the paper.

Acknowledgments

The authors acknowledge the financial support of the Biophysical Sciences Institute in Durham, a grant INCT-INBEQMeDI from CNPq, grant 2014/15546-1 from São Paulo Research Foundation (FAPESP). A FAPESP fellowship to AEZ (2013/20715-4) is also acknowledged. We thank the technical assistance and helpful discussions of Dra. Joci N. A. Macedo, Andressa A. Pinto, Derminda I. de Moraes, Yuri V. Santos, Prof. John Girkin and Prof. Richard C. Garratt.

References

- [1] L. Cao, X. Ding, W. Yu, X. Yang, S. Shen, L. Yu, Phylogenetic and evolutionary analysis of the septin protein family in metazoan, *FEBS Letters* 581 (2007) 5526-5532.
- [2] L. Hartwell, Genetic control of the cell division cycle in yeast. IV. Genes controlling bud emergence and cytokinesis., *Experimental Cell Research* 69 (1971) 265-276.
- [3] C.L. Beites, H. Xie, R. Bowser, W.S. Trimble, The septin CDCrel-1 binds syntaxin and inhibits exocytosis, *Nat. Neurosci.* 2 (1999) 434-439.

- [4] C.M. Field, Characterization of anillin mutants reveals essential roles in septin localization and plasma membrane integrity, *Development* 132 (2005) 2849-2860.
- [5] F. Caudron, Y. Barral, Septins and the Lateral Compartmentalization of Eukaryotic Membranes, *Developmental Cell* 16 (2009) 493-506.
- [6] M. Kinoshita, Diversity of septin scaffolds, *Current Opinion in Cell Biology* 18 (2006) 54-60.
- [7] S.K. Kim, A. Shindo, T.J. Park, E.C. Oh, S. Ghosh, R.S. Gray, R.A. Lewis, C.A. Johnson, T. Attie-Bittach, N. Katsanis, J.B. Wallingford, Planar Cell Polarity Acts Through Septins to Control Collective Cell Movement and Ciliogenesis, *Science* 329 (2010) 1337-1340.
- [8] T. Tada, A. Simonetta, M. Batterton, M. Kinoshita, D. Edbauer, M. Sheng, Role of Septin Cytoskeleton in Spine Morphogenesis and Dendrite Development in Neurons, *Current Biology* 17 (2007) 1752-1758.
- [9] L. Dolat, Q. Hu, E.T. Spiliotis, Septin functions in organ system physiology and pathology, *Biological Chemistry* 395 (2014).
- [10] P.A. Hall, S.E.H. Russell, The pathobiology of the septin gene family, *The Journal of Pathology* 204 (2004) 489-505.
- [11] A. Bertin, M.A. McMurray, P. Grob, S.S. Park, G. Garcia, I. Patanwala, H.I. Ng, T. Alber, J. Thorner, E. Nogales, *Saccharomyces cerevisiae* septins: Supramolecular organization of heterooligomers and the mechanism of filament assembly, *Proceedings of the National Academy of Sciences* 105 (2008) 8274-8279.
- [12] W. Garcia, N.C. Rodrigues, M.O. Neto, A.P.U. Araújo, I. Polikarpov, M. Tanaka, T. Tanaka, R.C. Garratt, The stability and aggregation properties of the GTPase domain from human SEPT4, *Biochimica et Biophysica Acta* 1784 (2008) 1720-1727.
- [13] J.C.P. Damalio, W. Garcia, J.N.A. Macêdo, I.A. Marques, J.M. Andreu, R. Giraldo, R.C. Garratt, A.P.U. Araújo, Self assembly of human septin 2 into amyloid filaments, *Biochimie* 94 (2012) 628-636.
- [14] M. Sirajuddin, M. Farkasovsky, F. Hauer, D. Kühlmann, I.G. Macara, M. Weyand, H. Stark, A. Wittinghofer, Structural insight into filament formation by mammalian septins, *Nature* 449 (2007) 311-315.
- [15] E. Zent, A. Wittinghofer, Human septin isoforms and the GDP-GTP cycle, *Biological chemistry* 395 (2014) 169-180.
- [16] M. Kinoshita, Assembly of Mammalian Septins, *Journal of Biochemistry* 134 (2003) 491-496.
- [17] M.E. Sellin, L. Sandblad, S. Stenmark, M. Gullberg, Deciphering the rules governing assembly order of mammalian septin complexes, *Molecular Biology of the Cell* 22 (2011) 3152-3164.
- [18] A.A. Bridges, M.S. Jentsch, P.W. Oakes, P. Occhipinti, A.S. Gladfelter, Micron-scale plasma membrane curvature is recognized by the septin cytoskeleton, *The Journal of Cell Biology* 213 (2016) 23-32.
- [19] A.A. Bridges, A.S. Gladfelter, Septin Form and Function at the Cell Cortex, *Journal of Biological Chemistry* 290 (2015) 17173-17180.
- [20] L.A. Nahum, M.M. Mourão, G. Oliveira, New Frontiers in *Schistosoma* Genomics and Transcriptomics, *Journal of Parasitology Research* 2012 (2012) 1-11.
- [21] A.E. Zeraik, G. Rinaldi, V.H. Mann, A. Popratiloff, A.P.U. Araujo, R. DeMarco, P.J. Brindley, Septins of Platyhelminths: Identification, Phylogeny, Expression and Localization among Developmental Stages of *Schistosoma mansoni*, *PLoS Neglected Tropical Diseases* 7 (2013) e2602.
- [22] A.E. Zeraik, V.E. Galkin, G. Rinaldi, R.C. Garratt, M.J. Smout, A. Loukas, V.H. Mann, A.P. Araujo, R. DeMarco, P.J. Brindley, Reversible paralysis of *Schistosoma*

mansoni by forchlorfenuron, a phenylurea cytokinin that affects septins, *Int J Parasitol* 44 (2014) 523-531.

- [23] S. Tayyab, S. Qamar, M. Islam, Size Exclusion Chromatography and Size Exclusion HPLC of Proteins, *Biochemical Education* 19 (1991) 149-152.
- [24] S.M. Kelly, T.J. Jess, N.C. Price, How to study proteins by circular dichroism, *Biochimica et Biophysica Acta (BBA) - Proteins & Proteomics* 1751 (2005) 119-139.
- [25] A.D. Ferrao-Gonzales, S.O. Souto, J.L. Silva, D. Foguel, The preaggregated state of an amyloidogenic protein: Hydrostatic pressure converts native transthyretin into the amyloidogenic state., *Proceedings of the National Academy of Sciences of the United States of America* 97 (2000) 6445– 6450.
- [26] R. Seckler, G.-M. Wug, S.N. Timasheff, Interactions of Tubulin with Guanylyl-(P-y-Methylene)diphosphonate: Formation and Assembly of a stoichiometric complex, *The Journal of Biological Chemistry* 13 (1990) 7655-7661.
- [27] A.E. Zeraik, H.M. Pereira, Y.V. Santos, J. Brandao-Neto, M. Spoerner, M.S. Santos, L.A. Colnago, R.C. Garratt, A.P.U. Araujo, R. DeMarco, Crystal structure of a *Schistosoma mansoni* septin reveals the phenomenon of strand slippage in septins dependent on the nature of the bound nucleotide, *Journal of Biological Chemistry* (2014).
- [28] J. Tellinghuisen, Isothermal titration calorimetry at very low c, *Analytical Biochemistry* 373 (2008) 395-397.
- [29] M.I. Angelova, D.S. Dimitrov, Liposome electroformation, *Faraday Discuss. Chem. Soc.* 81 (1986) 303-311.
- [30] J.T. Vivian, P.R. Callis, Mechanisms of Tryptophan Fluorescence Shifts in Proteins, *Biophysical Journal* 80 (2001) 2093-2109.
- [31] M. Biancalana, S. Koide, Molecular mechanism of Thioflavin-T binding to amyloid fibrils, *Biochimica et Biophysica Acta (BBA) - Proteins & Proteomics* 1804 (2010) 1405-1412.
- [32] M. Groenning, Binding mode of Thioflavin T and other molecular probes in the context of amyloid fibrils-current status, *Journal of Chemical Biology* 3 (2010) 1-18.
- [33] E. Zent, I. Vetter, A. Wittinghofer, Structural and biochemical properties of Sept7, a unique septin required for filament formation, *Biological Chemistry* 392 (2011).
- [34] Joci N.A. Macedo, Napoleão F. Valadares, Ivo A. Marques, Frederico M. Ferreira, Julio C.P. Damalio, Humberto M. Pereira, Richard C. Garratt, Ana P.U. Araujo, The structure and properties of septin 3: a possible missing link in septin filament formation, *Biochemical Journal* 450 (2013) 95-105.
- [35] E. Zent, A. Wittinghofer, Human septin isoforms and the GDP-GTP cycle, *Biological Chemistry* 395 (2014) 169-180.
- [36] J. Zhang, C. Kong, H. Xie, P.S. McPherson, S. Grinstein, W.S. Trimble, Phosphatidylinositol polyphosphate binding to the mammalian septin H5 is modulated by GTP, *Current Biology* 9 (1999) 1458–1467.
- [37] Y. Tanaka-Takiguchi, M. Kinoshita, K. Takiguchi, Septin-Mediated Uniform Bracing of Phospholipid Membranes, *Current Biology* 19 (2009) 140-145.
- [38] Y.-W. Huang, M.C. Surka, D. Reynaud, C. Pace-Asciak, W.S. Trimble, GTP binding and hydrolysis kinetics of human septin 2, *FEBS Journal* 273 (2006) 3248-3260.
- [39] I. de Almeida Marques, N.F. Valadares, W. Garcia, J.C. Damalio, J.N. Macedo, A.P. de Araujo, C.A. Botello, J.M. Andreu, R.C. Garratt, Septin C-terminal domain interactions: implications for filament stability and assembly, *Cell Biochem Biophys* 62 (2012) 317-328.

- [40] C. Martinez, M.A. Sanjuan, J.A. Dent, L. Karlsson, J. Ware, Human septin-septin interactions as a prerequisite for targeting septin complexes in the cytosol, *Biochem. J.* 382 (2004) 783–791.
- [41] V.H. Serrao, F. Alessandro, V.E. Caldas, R.L. Marcal, H.D. Pereira, O.H. Thiemann, R.C. Garratt, Promiscuous interactions of human septins: the GTP binding domain of SEPT7 forms filaments within the crystal, *FEBS Lett* 585 (2011) 3868-3873.
- [42] S. Sokalingam, G. Raghunathan, N. Soundrarajan, S.G. Lee, A study on the effect of surface lysine to arginine mutagenesis on protein stability and structure using green fluorescent protein, *PLoS One* 7 (2012) e40410.
- [43] W. Garcia, A.P.U. Araujo, F. Lara, D. Foguel, M. Tanaka, T. Tanaka, R.C. Garratt, An Intermediate Structure in the Thermal Unfolding of the GTPase Domain of Human Septin 4 (SEPT4/Bradeion-â) Forms Amyloid-like Filaments in Vitro, *Biochemistry* 46 (2007) 11101-11109.
- [44] A. Bertin, M.A. McMurray, P. Grob, S.S. Park, G. Garcia, 3rd, I. Patanwala, H.L. Ng, T. Alber, J. Thorner, E. Nogales, *Saccharomyces cerevisiae* septins: supramolecular organization of heterooligomers and the mechanism of filament assembly, *Proc Natl Acad Sci U S A* 105 (2008) 8274-8279.
- [45] C.L. Beites, K.A. Campbell, W.S. Trimble, The septin Sept5/CDCrel-1 competes with alpha-SNAP for binding to the SNARE complex, *Biochem J* 385 (2005) 347-353.
- [46] E. Tokhtaeva, J. Capri, E.A. Marcus, J.P. Whitelegge, V. Khuzakhmetova, E. Bukharaeva, N. Deiss-Yehiely, L.A. Dada, G. Sachs, E. Fernandez-Salas, O. Vagin, Septin Dynamics Are Essential for Exocytosis, *Journal of Biological Chemistry* 290 (2015) 5280-5297.
- [47] H. Ito, K. Atsuzawa, R. Morishita, N. Usuda, K. Sudo, I. Iwamoto, K. Mizutani, R. Katoh-Semba, Y. Nozawa, T. Asano, K. Nagata, Sept8 controls the binding of vesicle-associated membrane protein 2 to synaptophysin, *J Neurochem* 108 (2009) 867-880.